

See discussions, stats, and author profiles for this publication at: <https://www.researchgate.net/publication/23413530>

# Chitosan-Modified Poly(acrylonitrile-co-acrylic acid) Nanofibrous Membranes for the Immobilization of Concanavalin A

ARTICLE in BIOMACROMOLECULES · NOVEMBER 2008

Impact Factor: 5.75 · DOI: 10.1021/bm800882z · Source: PubMed

---

CITATIONS

28

READS

101

## 5 AUTHORS, INCLUDING:



Zhen-Mei Liu

Institute of Biomaterials and Biomedical E...

30 PUBLICATIONS 977 CITATIONS

[SEE PROFILE](#)



Xiao-jun Huang

Zhejiang University

60 PUBLICATIONS 1,458 CITATIONS

[SEE PROFILE](#)



Zhi-Kang Xu

Zhejiang University

251 PUBLICATIONS 6,271 CITATIONS

[SEE PROFILE](#)

# Chitosan-Modified Poly(acrylonitrile-co-acrylic acid) Nanofibrous Membranes for the Immobilization of Concanavalin A

Ai-Fu Che, Zhen-Mei Liu, Xiao-Jun Huang, Zhen-Gang Wang, and Zhi-Kang Xu\*

*Institute of Polymer Science, and Key Laboratory of Macromolecular Synthesis and Functionalization (Ministry of Education), Zhejiang University, Hangzhou 310027, PR China*

Received August 6, 2008; Revised Manuscript Received October 1, 2008

Lectin affinity membranes have been receiving much attention for the separation and detection of various glycoconjugates. In this work, we present a simple and efficient method for the preparation of lectin affinity nanofibrous membranes. Chitosan-modified poly(acrylonitrile-*co*-acrylic acid) (PANCAA) nanofibrous membranes were first prepared by a coupling reaction between the primary amino groups of chitosan and the carboxyl groups of PANCAA electrospun membranes. Surface characterizations by attenuated total reflectance Fourier transform infrared spectroscopy (FT-IR/ATR), X-ray photoelectron spectroscopy (XPS) and field-emission scanning electron microscopy (FESEM) confirm the chemical and morphological changes of the studied nanofibrous membranes. Fluorescence-labeled concanavalin A (FL-Con A) was then immobilized on these membranes via noncovalent binding. Analyses by fluorescence spectrophotometer (FS) and confocal laser scanning microscopy (CLSM) reveal that the immobilization of Con A onto the modified nanofibrous membranes has been successfully achieved on the basis of the electrostatic interaction and the specific recognition between Con A and chitosan. The results show that the amount of adsorbed FL-Con A increases dramatically with the increasing coupling degree of chitosan (CDC) on the nanofibrous membrane. Moreover, Con A immobilized on the chitosan-modified nanofibrous membranes (CMNMs) can remain relatively stable at pH 5.3. Therefore, it is believed that this work may provide a new kind of material for affinity application.

## Introduction

Plant lectins are proteins that have been proven to be valuable for the separation or detection of glycoconjugates (e.g., glycoproteins, glycopeptides, and glycolipids) on the basis of the specific association of the saccharide–protein complex that is often emerged on the cell surface.<sup>1,2</sup> Plant lectins can be immobilized as affinity ligands on matrices for so-called lectin affinity chromatography, which has been well documented and has received much attention in recent years.<sup>3</sup> The agarose-based column chromatography<sup>4,5</sup> was first studied for use.<sup>4,5</sup> However, it is often restricted to the laboratory scale because of resin deformation and bed solidification over time. Therefore, other matrices are used, which range from agarose to silica,<sup>6,7</sup> polymer beads,<sup>8,9</sup> and membranes,<sup>2,10–12</sup> out of which membrane-based affinity chromatography has drawn more attention because of its distinct characteristics such as low pressure drop, high flowing rate, high productivity, and easy scale-up.<sup>13–16</sup> Therefore, lectin affinity membrane chromatography would be of great importance for potential applications.

An ideal matrix for membrane chromatography should possess a porous structure with physicochemical stability under harsh conditions, a hydrophilic surface for preventing nonspecific binding, and reactive groups for further coupling of functional ligands.<sup>14</sup> Both natural and synthetic polymers<sup>2,17,18</sup> that have excellent biocompatibility with lectin ligands were developed for the fabrication of lectin affinity membranes. In the pioneer work, commercially available cellulose-derived microporous membranes<sup>12</sup> were studied for the immobilization of Con A. Con A is one of the most often studied lectins and has shown strong affinity for α-D-mannose and α-D-glucose as well as *N*-acetyl-D-glucosamine.<sup>19–23</sup> However, the relatively

small pore size limited their application in chromatography. As an alternative, macroporous membranes were developed and proved to be more efficient.<sup>2,10,11,24</sup> Recently, electrospinning has been considered as a useful method for preparing nonwoven fabrics of submicron or nanoscale fibers. The especially high porosity and large surface-to-area ratio of electrospun nanofibrous membrane make it superior for affinity separation.<sup>25</sup>

Chitosan is one of the most widely biomacromolecules after cellulose because of its unique properties such as biodegradability, antibacterial and antifungal activity, and wound healing acceleration.<sup>26</sup> Besides its ubiquitous availability, the affinity interaction with lectins makes it a good candidate for lectin affinity chromatography.<sup>27</sup> Taking this into account, electrospinning of chitosan<sup>28–30</sup> could be an alternative approach for preparing lectin affinity membranes. However, the common solvent for chitosan is usually volatile and caustic, which makes the electrospinning process troublesome and unsafe. Therefore, the coupling of chitosan onto nanofibrous membranes, which combines the merits of high porosity and strong affinity with lectin, may be superior for the preparation of lectin affinity membrane.

In this article, chitosan was covalently tethered onto the nanofibrous membranes electrospun from PANCAA, followed by the immobilization of Con A. The process is schematically shown in Figure 1. The interaction mechanisms of Con A and CMNM were preliminarily studied on the basis of the adsorption and desorption experiments.

## Materials and Methods

**Materials.** PANCAA with an average molecular weight of  $2.4 \times 10^5$  g/mol and an acrylic acid content of 15.3 mol % was synthesized by free radical polymerization in dimethyl sulfoxide (DMSO).<sup>31</sup> DMSO and *N,N*-dimethylformamide (DMF) were commercially obtained from

\* Corresponding author. E-mail: xuzk@zju.edu.cn.

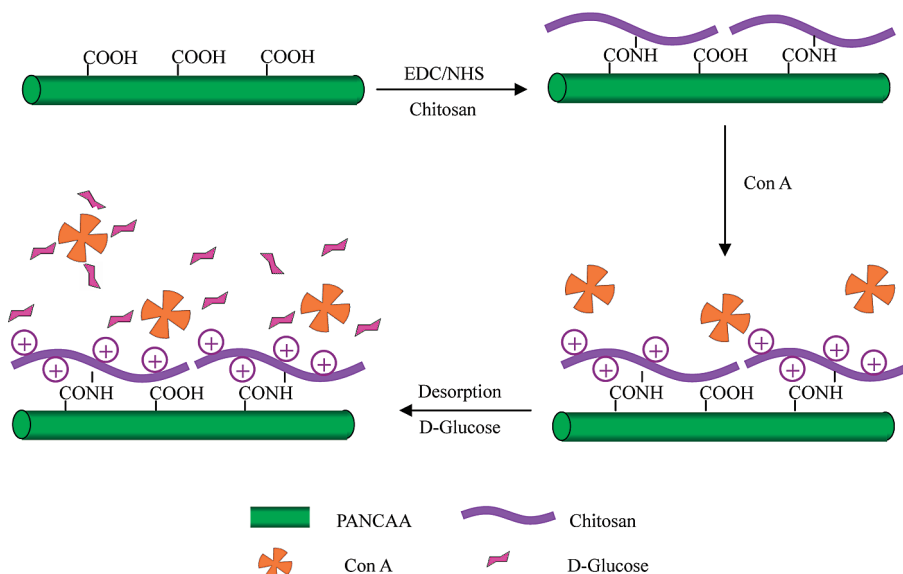


**Figure 1.** Schematic representation of the whole experimental process.

Shanghai Chemical Agent (China) and were purified by distillation under vacuum before use. 1-Ethyl-3-(dimethyl-aminopropyl) carbodiimide hydrochloride (EDC) was purchased from Shanghai Medpep (China), and *N*-hydroxysuccinimide (NHS) was purchased from Sigma. 2-[4-(2-Hydroxyethyl)-1-piperazinyl] ethanesulfonic acid (HEPES) was a commercial product of Nanjing Robiot (China) and was used as received. Chitosan was obtained from Shanghai Aobo Biotechnology (China). Fluorescence-labeled Con A (FL-Con A) was purchased from Vector Laboratories. D-Glucose (analytical grade) was delivered by Chemical Reagent Company (China) and used without further purification. All other chemicals were of analytical grade and were used as received.

**Electrospinning of Poly(acrylonitrile-*co*-acrylic acid).** PANCAA was dissolved in DMF at room temperature with gentle stirring for 12 h to form homogeneous solutions of various concentrations. After the air bubbles were completely removed, PANCAA solution was poured into a plastic syringe that was held on self-made electrospinning equipment. The feeding rate was controlled by a microinfusion pump (WZ-50C2, Zhejiang University Medical Instrument, China). The electric field supported by a high-voltage power supply (GDW-a, Tianjin Dongwen High-Voltage Power Supply Plant, China) with a current output of 0.000 to 0.001 mA was generated between a stainless steel needle (inner diameter 1.2 mm) at the end of the syringe and a ground collector (aluminum sheet on a flat glass). The electrospinning process was performed between the needle tip and the collector at 28 °C with 45% relative humidity. It took ca. 4 h to obtain a sufficiently thick nanofibrous membrane for further studies. The resultant membrane was dried under vacuum at 80 °C to remove the residual solvent.

**Coupling of Chitosan on Poly(acrylonitrile-*co*-acrylic acid) Nanofibrous Membrane.** Chitosan with a low molecular weight (LMWC, with deacetylation degree of 84% and  $M_w$  of 7000 Da) was prepared by a H<sub>2</sub>O<sub>2</sub> oxidative degradation method, as previously described.<sup>32</sup> The yield calculated by the mass ratio of the LMWC to the original chitosan was ~80 wt %.

A certain mass of PANCAA nanofibrous membrane was thoroughly washed with acetic acid buffer solution (AABS, 50 mM, pH 5.0). Subsequently, the membrane was taken out, wiped with filter papers, and submerged in an EDC/NHS solution (5 and 10 mg/mL in AABS, respectively; 1:1 molar ratio of EDC to NHS) with gentle vibration for 2.5 h at 25 °C. The activated membrane was washed several times with AABS and dipped into LMWC solution. The coupling reaction was carried out at 25 °C for 20 and 44 h, respectively. The resulting membrane was washed several times with 1.0 vol % acetic acid solution to remove the residual chitosan adsorbed on the membrane surface and was then rinsed with a large excess of deionized water to remove the

residual acetic acid. Finally, the CMNM was submerged into ethanol for 20 min and dried under vacuum for 24 h at 40 °C. The chitosan-modified PANCAA dense films were prepared under the same experimental conditions.

The CDC (wt %) was calculated by the following equation:

$$\text{CDC} = \frac{W_1 - W_0}{W_0} \quad (1)$$

where  $W_0$  and  $W_1$  are the masses of the nanofibrous membrane before and after the coupling, respectively.

**Fluorescence-Labeled Concanavalin A Immobilization.** FL-Con A (labeled by fluorescein isothiocyanate) was used as a fluorescent probe in our work to evaluate the affinity interaction between Con A and CMNMs. All operations were carried out in a dark room. FL-Con A (5 g/L) was diluted to 0.2 g/L using HEPES buffer solution (pH 5.3 and 7.5, 10 mM) supplemented with 0.1 mM Ca<sup>2+</sup>, 0.01 mM Mn<sup>2+</sup>, and 0.15 M Na<sup>+</sup>. Samples of 0.05 mg nanofibrous membranes were added to the 96-well cell culture plate filled with 200 μL of FL-Con A solution. Then, the mixtures were incubated at 25 °C. After 2 h, the nanofibrous membranes were taken out and washed with HEPES buffer solution several times to remove the free FL-Con A. Subsequently, the nanofibrous membranes were dried under vacuum at 25 °C for 2 h.

To further evaluate the stability of the adsorbed Con A on the CMNMs, we used D-glucose in HEPES buffer solution (pH 5.3 and 7.5) to remove FL-Con A from the nanofibrous membranes surface. After adsorption, the nanofibrous membranes were washed and wiped with filter papers and were then put in another 96-well cell culture plate by incubation with 200 μL of D-glucose solution (HEPES, pH 5.3 and 7.5) at 25 °C for 24 h. Finally, the nanofibrous membranes were taken out and washed with HEPES buffer solution several times. All of the washing solutions were collected and diluted to 3 mL in a glass tube. The nanofibrous membranes were dried under vacuum at 25 °C for 2 h. A fluorescence spectrophotometer (FS, Shimadzu RF-3510PC, Japan) was used to get fluorescence spectra of the desorbed solutions using matched quartz cells of 1 cm path length.

**Surface Characterization.** To confirm the chemical and morphological changes on the surface of PANCAA nanofibrous membrane, we used FT-IR/ATR, XPS, FESEM, WCA, SSFS, and CLSM.

FT-IR/ATR spectra were acquired with a Vector 22 FT-IR spectrometer (Bruker Optics, Switzerland) equipped with an ATR accessory (KRS-5 crystal, 45°). For each spectrum, 32 scans were taken at a resolution of 2 cm<sup>-1</sup>.

XPS measurements were carried out on an RBD upgraded PHI-5000C ESCA system (Perkin-Elmer) with Mg K $\alpha$  radiation ( $\hbar\nu$  =

1253.6 eV). The survey spectra and the core-level spectra with much higher resolution were both recorded using an RBD 147 interface (RBD Enterprises) controlled by the Auger Scan 3.21 software. Binding energies were calibrated with the containment carbon (C 1s = 284.6 eV). The data analysis was carried out on the RBD Auger Scan 3.21 software provided by RBD Enterprises or the XPS Peak 4.1 software provided by Raymund W. M. Kwok (The Chinese University of Hongkong, China).

The morphology of the native and modified nanofibrous membranes was examined under FESEM (SIRION-100, FEI, Netherlands) after the samples were spayed with a gold layer.

A CTS-200 contact angle system (Mighty Technology, China) was used to determine the static contact angle by sessile drop method at room temperature. A water drop ( $\sim 2 \mu\text{L}$ ) was loaded on the membrane surface from a needle tip. All results were an average of five measurements.

SSFS measurements were carried out on an FS (Shimadzu RF-3510PC, Japan) equipped with a solid sample holder accessory (P/N 204-26836-01). The cell plane where the nanofibrous membranes were fixed was set at  $45^\circ$  to the excitation beam. The fluorescence emission at 500–600 nm was measured with an excitation light of 488 nm and a bandwidth of 5 nm.

High-resolution images for the nanofibrous membranes after FL-Con A adsorption were also obtained by CLSM (Leica Microsystems, Wetzlar, Germany) with  $2048 \times 2048$  pixels. The 488 nm line of an argon-ion laser excited the fluorescing materials. The filters in the experimental setup were chosen to allow the measurement of the fluorescence at 500–535 nm. Meanwhile, the relative fluorescence intensity was quantitatively analyzed using a  $20 \times$  NA 0.7 dry objective and the xyz scan mode at 2% laser power. For each sample, 10 positions were randomly selected for the measurements. Native PANCAA nanofibrous membrane was used as a control. The desorption percent (DP) of FL-Con A was calculated according to the following equation

$$\text{DP}(\%) = \frac{I_A - I_D}{I_A} \times 100\% \quad (2)$$

where  $I_A$  and  $I_D$  represent the relative fluorescence intensities of the adsorbed and the desorbed nanofibrous membranes, respectively.

## Results and Discussion

**Preparation and Characterization of Chitosan-Modified Nanofibrous Membranes.** For the preparation of PANCAA nanofibrous membrane with ideal fiber structures suitable for the coupling of chitosan, several important electrospinning parameters such as solution concentration, electrical field strength, and feeding rate were discussed previously.<sup>31</sup> The results demonstrate that the optimized conditions should be a 5 wt % concentration of polymer solution, a feeding rate of 1.0 mL/h, and an electric field strength of 12.0 kV at a nozzle-to-collector distance of 15 cm under the same ambient conditions. Consequently, PANCAA electrospun membranes composed of nanofibers with an average diameter of  $190 \pm 23$  nm were fabricated.

Chitosan is a kind of cationic polysaccharide that possesses several prominent characteristics such as hydrophilicity, biocompatibility, biodegradability, and antibacterial properties. However, the poor solubility of the common chitosan limits its further application. As a comparison, LMWC can be facilely resolved in the buffer solution.<sup>33</sup> Herein, LMWC was obtained by a  $\text{H}_2\text{O}_2$  oxidative degradation method.<sup>32</sup> Surface modification of PANCAA nanofibrous membrane with LMWC was achieved using EDC and NHS as coupling agents. The results show that the CDC is strongly dependent on the reaction conditions, that is, EDC concentration and the reaction time, as listed in Table 1. With increased EDC concentration or extended reaction time,

**Table 1.** CDCs of Chitosan-Modified PANCAA Nanofibrous Membranes

sample <sup>a</sup>	reaction conditions		CDC (wt %) <sup>b</sup>	contact angles (deg) <sup>c</sup>
	concn of EDC (mg/mL)	reaction time (h)		
PANCAA-CS1	5	20	$6.62 \pm 0.98$	$65.6 \pm 1.7$
PANCAA-CS2	10	20	$10.8 \pm 1.21$	$64.5 \pm 1.8$
PANCAA-CS3	10	44	$20.7 \pm 1.36$	$63.8 \pm 1.5$

<sup>a</sup> PANCAA-CS1, 2, and 3 represent the chitosan-modified PANCAA nanofibrous membranes with different CDCs. <sup>b</sup> Data are expressed as the mean  $\pm$  SD of three independent measurements. <sup>c</sup> Data are expressed as the mean  $\pm$  SD of five independent measurements.

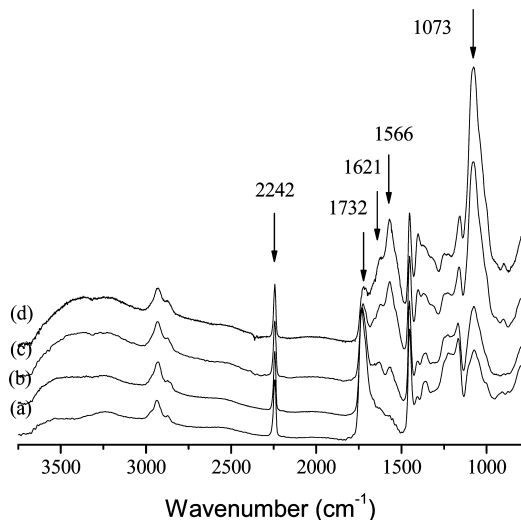


**Figure 2.** FT-IR/ATR spectra of the studied nanofibrous membranes (a) PANCAA, (b) PANCAA-CS1, (c) PANCAA-CS2, and (d) PANCAA-CS3.

the CDC is highly increased. The resulting nanofibrous membranes with different CDCs are simply denoted as PANCAA-CS1, PANCAA-CS2, and PANCAA-CS3.

FT-IR/ATR spectra were used to confirm the occurrence of surface modification. For native PANCAA (Figure 2a), the absorption peak at  $2242 \text{ cm}^{-1}$  is derived from the  $\text{C}\equiv\text{N}$  stretching vibration, and the one at  $1732 \text{ cm}^{-1}$  is ascribed to the  $\text{C}=\text{O}$  stretching vibration. The characteristic peak at  $1073 \text{ cm}^{-1}$  is assigned to a  $\text{C}-\text{O}$  stretching vibration. After modification with chitosan, as shown in Figure 2b–d, two striking characteristic peaks appear at  $1566$  and  $1621 \text{ cm}^{-1}$ , which are assigned to the  $\text{N}-\text{H}$  bending vibration of  $-\text{NH}_2$  groups and that of  $-\text{CONH}-$  groups introduced by the coupling reaction, respectively. Meanwhile, the absorption peak at  $1732 \text{ cm}^{-1}$  is gradually weakened and slightly shifts to  $1726 \text{ cm}^{-1}$  with the increase in CDC on the surface of the nanofibrous membrane. Furthermore, the intensity of the absorption band in the range of  $3100$  and  $3700 \text{ cm}^{-1}$  and the peak at  $1073 \text{ cm}^{-1}$  obviously increase.

XPS was applied to characterize the chemical composition on the nanofibrous membrane surface. For comparison, the XPS spectrum of chitosan powder was also taken. For both the native PANCAA nanofibrous membrane and chitosan powder, three peaks dominate, which are ascribed to the binding energy of C 1s (284.6 eV), O 1s (531.4 eV), and N 1s (398.6 eV) (Figure 3a,e). The peak that corresponds to the oxygen element from chitosan is much stronger than that from PANCAA. After chitosan coupling, the intensities of C 1s and N 1s become weaker, whereas the intensity of O 1s gradually increases, especially for PANCAA-CS3, which has the highest CDC.

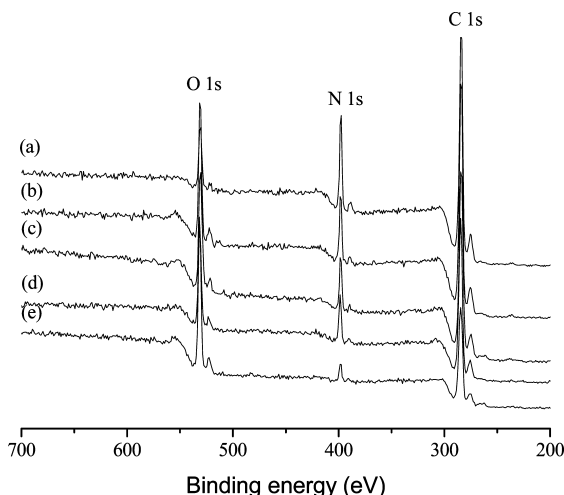


**Figure 3.** Survey XPS spectra of the studied nanofibrous membranes (a) PANCAA, (b) PANCAA-CS1, (c) PANCAA-CS2, and (d) PANCAA-CS3 and (e) chitosan powder.

**Table 2.** Data Analysis of Chemical Compositions of the Native and Chitosan-Modified PANCAA Nanofibrous Membranes by XPS

sample	C%	O%	N%	O/N
PANCAA	79.07	7.18	13.75	0.522
PANCAA-CS1	75.76	14.33	9.92	1.445
PANCAA-CS2	75.14	15.34	9.27	1.655
PANCAA-CS3	74.65	16.31	9.03	1.806
chitosan	63.96	28.95	7.11	4.072

These can be explained by the chemical differences between chitosan and PANCAA. Compared with the native PANCAA nanofibrous membrane, the mole content of the oxygen element in chitosan is higher, whereas that for the carbon or nitrogen element is relatively lower. As a result, the mole ratio of O to N (O/N) on the surface of CMNNs increases with the CDC. The corresponding data are listed in Table 2.

Typical FESEM images of the CMNNs are shown in Figure 4. Compared with the native PANCAA sample, the modified nanofibrous membranes become a bit looser. However, the nanofiber diameters do not change much with the single fiber remaining in the membrane. The results indicate that this PANCAA nanofibrous membrane is a stable carrier for surface modification.

The hydrophilicity/hydrophobicity of the membrane surfaces before and after the coupling was evaluated by WCA measurement. Because the high porosity of the nanofibrous membrane would interfere with WCA measurements, chitosan-modified PANCAA dense films were prepared under the same conditions. As shown in Table 1, the WCAs of chitosan-modified surfaces are slightly lower than that of the pure PANCAA surface ( $67.7 \pm 1.9$ ). This result indicates that the chitosan-modified surfaces are relatively hydrophilic, which facilitates the lectin immobilization.

**Noncovalent Immobilization of Concanavalin A on Chitosan-Modified Nanofibrous Membranes.** SSFS was used to measure the fluorescence intensities of different nanofibrous membranes after FL-Con A adsorption. Under the excitation wavelength of 488 nm, the emitted fluorescence intensities at 500–600 nm were counted (Figure 5). The fluorescence intensity shows that FL-Con A can be physically adsorbed on the native PANCAA nanofibrous membrane. However, the fluorescence intensity of the CMNM increases remarkably with the increase in CDC. Especially in the case of sample PANCAA-CS3, a sharp emission peak appears at 520 nm. It is known that solid-surface fluorescence is a sensitive and reliable method

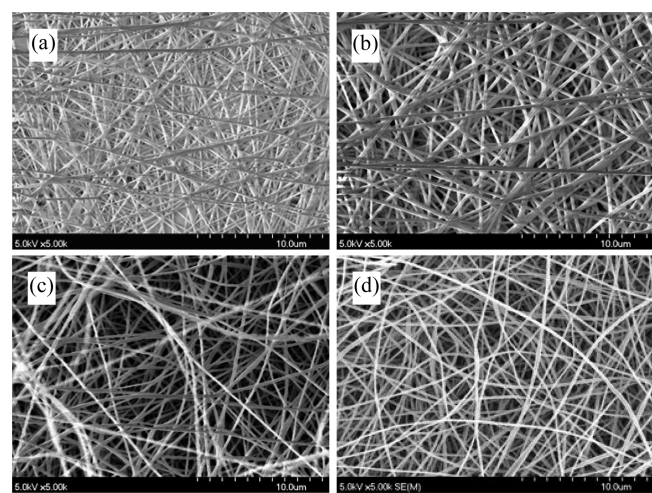


**Figure 4.** FESEM images of the studied nanofibrous membranes (a) PANCAA, (b) PANCAA-CS1, (c) PANCAA-CS2, and (d) PANCAA-CS3.

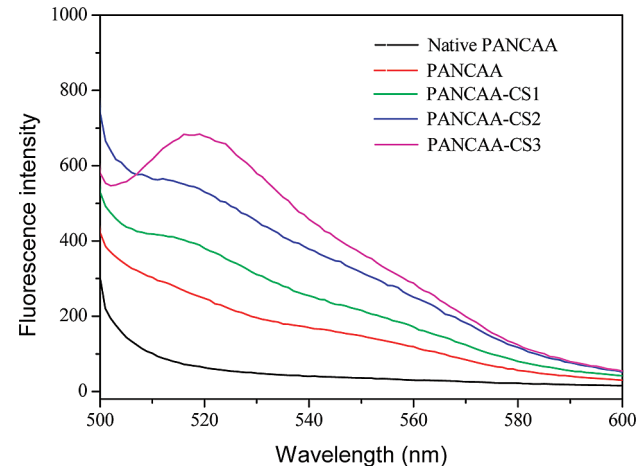


**Figure 5.** Typical SSFS spectra of the nanofibrous membranes with FL-Con A adsorption at pH 5.3.

for evaluating the fluorescence intensity of organic and inorganic solid surfaces at room temperature. Compared with the emission efficiency of the solution from the same chemical, the higher emission efficiency that resulted from the solid surface can be expected because the excited molecules are isolated and collision-restricted.<sup>34–37</sup> Therefore, it can simply serve as a semiquantitative method for determining the relative amount of fluorescence substance on the solid surface. The results provide positive evidence of the presence of strong interactions between FL-Con A and chitosan coupled on the surface of the nanofibrous membrane.

Fluorescent images and relative fluorescence intensities of the nanofibrous membranes after FL-Con A adsorption were obtained by CLSM. These can be used to characterize the distribution of FL-Con A on the surface of CMNNs and are helpful for further quantitative analysis. Figures 6 and 7 show the results of CLSM. From the high-resolution images in Figure 6, it is found the nanofibrous membranes exhibit green color when excited at 488 nm which comes from the adsorbed FL-Con A, which indicate that FL-Con A uniformly covers the nanofiber surface and distributes evenly throughout the nanofibrous membrane. Moreover, as the CDC increases, the stronger color corresponds to the increase of adsorbed FL-Con A.

Relative fluorescence intensities were evaluated by CLSM for various samples, as illustrated in Figure 7. It can be seen

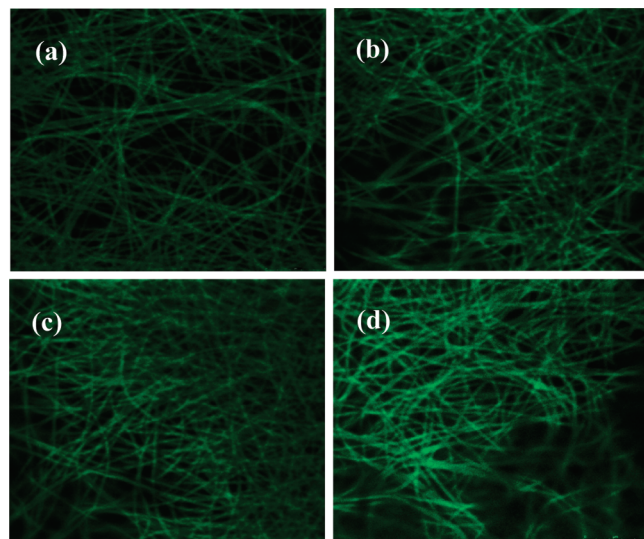


**Figure 6.** CLSM images of the nanofibrous membranes with FL-Con A adsorption at pH 5.3. (a) PANCAA, (b) PANCAA-CS1, (c) PANCAA-CS2, and (d) PANCAA-CS3.

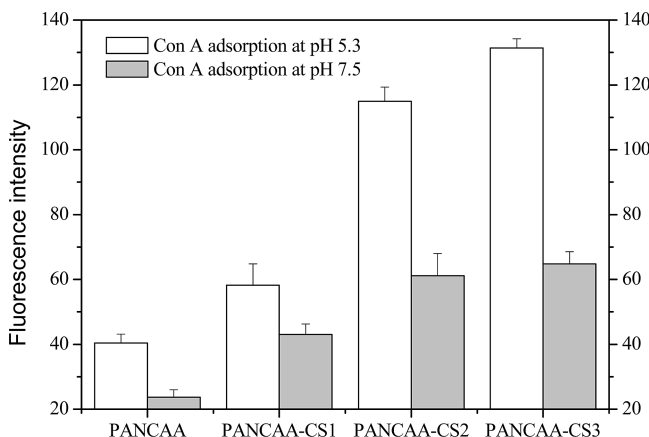


**Figure 7.** Comparison of the mean fluorescence intensity after FL-Con A adsorption at different pHs. Data are expressed as the mean  $\pm$  SD of three independent measurements.

that the CMNNMs adsorb more FL-Con A compared with the PANCAA nanofibrous membrane. As the CDC increases, the adsorbed amount increases accordingly, which is in agreement with the results in Figure 5.

**Possible Immobilization Mechanisms of Concanavalin A on Chitosan-Modified Nanofibrous Membranes.** The previous results demonstrate that the affinity interaction between Con A and chitosan obviously promotes the adsorption of Con A onto CMNNMs. Generally, chitosan is a kind of cationic polysaccharide that contains a great number of D-glucosamine groups in the main chain, which may be positively charged and interact with Con A through electrostatic interaction. The specific recognition interaction between N-acetyl-D-glucosamine groups and Con A has been confirmed by Gümüşderelioglu et al.<sup>19,27</sup> Therefore, the affinity interaction between LMWC tethered on the nanofibrous membranes and Con A may be a combination of electrostatic interaction and specific recognition in our work.

Taking these into accounts, we designed a series of adsorption and desorption experiments at both pH 5.3 and 7.5 to clarify the binding mechanism. It is found that the adsorption process is significantly dependent on pH, and a higher amount of adsorbed FL-Con A is acquired at pH 5.3 (Figure 7). As we know, the  $pK_a$  value of chitosan is 6.3 to 7.0,<sup>38</sup> and the

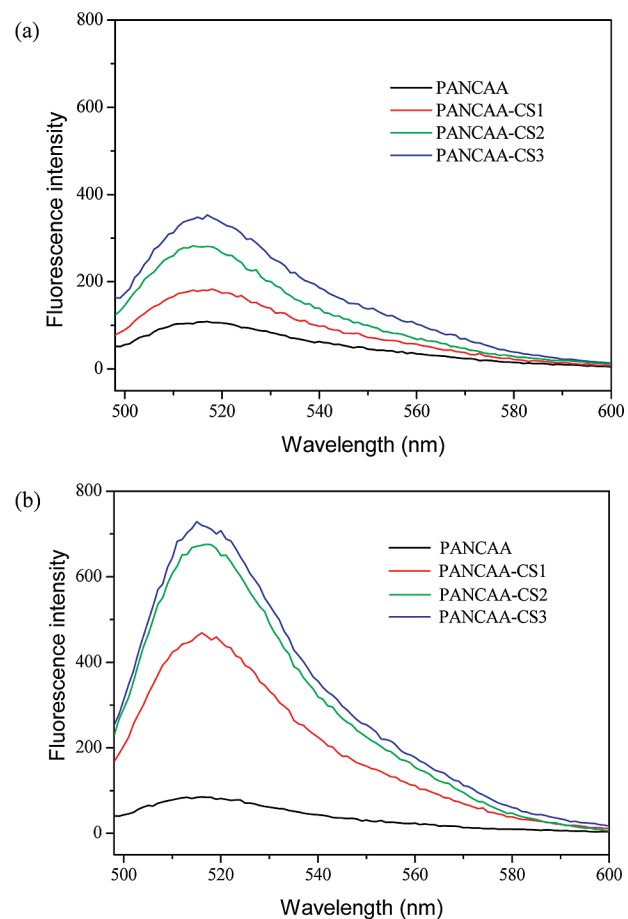


**Figure 8.** Fluorescence spectra of the desorbed solutions after desorption with 1 M D-glucose solution at (a) pH 5.3 and (b) pH 7.5.

isoelectric point of Con A is  $\sim$ 5. This means that at pH 5.3, chitosan is positively charged and can interact with negatively charged Con A through strong electrostatic interaction, whereas at pH 7.5, the electrostatic interaction is much weaker. However, it has been confirmed that the maximum binding capacity of Con A appeared at around pH 7.0 simply on the basis of the specific recognition.<sup>39,40</sup> Therefore, it is deduced that the electrostatic interaction plays a major role at pH 5.3, whereas the specific recognition is dominant at pH 7.5.

D-Glucose is one of the most common eluents for Con A desorption. The fluorescence spectra of the desorbed solutions are shown in Figure 8. It can be seen that for desorption conducted at both pH values, the fluorescence intensity is very weak for the native PANCAA nanofibrous membrane, whereas that for CMNNMs is strong, especially at pH 7.5.

Correspondingly, relative fluorescence intensities of the desorbed nanofibrous membranes were also measured by CLSM. The calculated results are illustrated in Figure 9. It is found that the FL-Con A on CMNNMs cannot be desorbed thoroughly by D-glucose, and the DP at pH 5.3 (<30%) is comparatively lower than that at pH 7.5 (close to 50%). This can be ascribed to the following two reasons. First, the affinity interaction of Con A–chitosan is multivalent with a binding constant ( $K_a = 1.0 \times 10^5 \text{ M}^{-1}$ ),<sup>27</sup> whereas the interaction of Con A–D-glucose is only monovalent ( $K_a = 0.8 \times 10^3 \text{ M}^{-1}$ ).<sup>41,42</sup> The much higher  $K_a$  confirms that the affinity interaction between Con A and chitosan on the nanofibrous membrane surface is stronger than that between Con A and D-glucose, resulting in a large number of Con A remaining. Furthermore, with increasing CDC, because

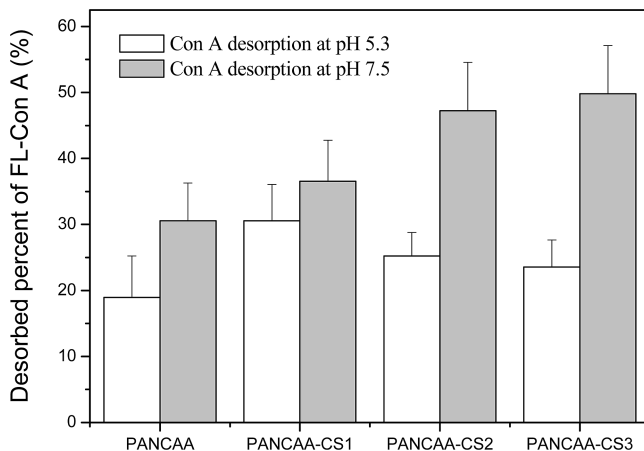


**Figure 9.** Comparison of the desorption percent of FL-Con A at different pHs. Data are expressed as the mean  $\pm$  SD of three independent measurements.

of the large availability of chitosan, the multivalent cooperative interaction may become stronger (pH 5.3). Second, the higher DP at pH 7.5 is mainly due to the weak electrostatic interaction, which is in accordance with the results in Figure 8. On the basis of the strong affinity interaction between FL-Con A and CMNNs at pH 5.3, Con A affinity nanofibrous membrane is considered to be a relatively stable lectin affinity membrane for the separation and detection of glycoconjugates.

## Conclusions

Electrospun membrane is an alternative carrier material for affinity separation of biomacromolecules because of its high porosity and large surface-to-area ratio. Con A affinity nanofibrous membrane was successfully prepared by the immobilization of Con A on CMNM on the basis of the electrostatic interaction and specific recognition between Con A and chitosan in this work. Chitosan was first covalently tethered onto PANCAA nanofibrous membranes using EDC/NHS as coupling agents. It is found that the CDC increases with increasing EDC concentration or extending reaction time. CMNNs with different CDCs were prepared for comparison. FT-IR/ATR and XPS confirm the chemical structures of CMNNs. FESEM images show the fine nanostructures of the electrospun nanofibers before and after the chitosan coupling, which implies that CMNM is a superior matrix. Con A was then immobilized on CMNM through noncovalent immobilization. SSFS and CLSM characterizations demonstrate that Con A is evenly distributed on the membrane surface, and the amount of adsorbed Con A correspondingly increases with the CDC. Furthermore, the interaction mechanisms were preliminarily studied by the adsorption and desorption experiments at pH 5.3 and 7.5. The results reveal that the electrostatic interaction plays a major role at pH 5.3, whereas the specific recognition is dominant at pH 7.5. The desorption process with D-glucose further demonstrates that the Con A affinity nanofibrous membrane exhibits relative stability. Therefore, it is believed that Con A affinity nanofibrous membrane is an excellent lectin affinity membrane for potential application in the separation and detection of glycoconjugates.

**Acknowledgment.** We are grateful for the financial support from the National Natural Science Foundation of China for Distinguished Young Scholars (to Z.-K.X., grant no. 50625309) and the National Natural Science Foundation of China (grant no. 20774080).

## Appendix

### Abbreviations

AABS,	acetic acid buffer solution
FT-IR/ATR,	attenuated total reflectance Fourier transform infrared spectroscopy
CMNM,	chitosan-modified nanofibrous membrane
PANCAA-CS,	chitosan-modified PANCAA nanofibrous membrane
LMWC,	chitosan with a low molecular weight
Con A,	concanavalin A
CLSM,	confocal laser scanning microscopy
CDC,	coupling degree of chitosan
DP,	desorption percent
DMF,	N,N-dimethylformamide
DMSO,	dimethyl sulfoxide
EDC,	1-ethyl-3-(dimethyl-aminopropyl) carbodiimide hydrochloride
FESEM,	field-emission scanning electron microscopy
FL-Con A,	fluorescence-labeled concanavalin A
FS,	fluorescence spectrophotometer
HEPES,	2-[4-(2-hydroxyethyl)-1-piperazinyl] ethanesulfonic acid
NHS,	N-hydroxysuccinimide
PANCAA,	poly(acrylonitrile- <i>co</i> -acrylic acid)
XPS,	X-ray photoelectron spectroscopy
SSFS,	solid surface fluorescence spectroscopy
WCA,	water contact angle

### References and Notes

- Liu, S. Q.; Wang, K. W.; Du, D.; Sun, Y. M.; He, L. *Biomacromolecules* **2007**, 8, 2142–2148.
- Rosenfeld, H.; Aniulyte, J.; Helmholz, H.; Liesiene, J.; Thiesen, P.; Niemeyer, B.; Prange, A. *J. Chromatogr., A* **2005**, 1092, 76–88.
- Monzo, A.; Bonn, G. K.; Guttmann, A. *Trends Anal. Chem.* **2007**, 26, 423–432.
- Davey, M. W.; Sulkowski, E.; Carter, W. A. *Biochemistry* **1974**, 15, 704–713.
- Santori, F.; Hubble, J. *J. Chromatogr., A* **2003**, 1003, 123–126.
- Helmholz, H.; Cartellieri, S.; He, L. Z.; Thiesen, P.; Niemeyer, B. *J. Chromatogr., A* **2003**, 1006, 127–135.
- Madera, M.; Mechref, Y.; Novotny, M. V. *Anal. Chem.* **2005**, 77, 4081–4090.
- Bahar, T.; Tuncel, A. *J. Appl. Polym. Sci.* **2004**, 92, 2116–2124.
- Bereli, N.; Akgol, S.; Yavuz, H.; Denizli, A. *J. Appl. Polym. Sci.* **2005**, 97, 1202–1208.
- Ruckenstein, E.; Guo, W. *Biotechnol. Prog.* **2004**, 20, 13–25.
- Kökpınar, Ö.; Harkensee, D.; Kasper, C.; Schepel, T.; Zeidler, R.; Reif, O. W.; Ulber, R. *Biotechnol. Prog.* **2006**, 22, 1215–1219.
- Mellado, M. C. M.; Curbelo, D.; Nobrega, R.; Castilho, L. R. *J. Chem. Technol. Biotechnol.* **2007**, 82, 636–645.
- Roper, D. K.; Lightfoot, E. N. *J. Chromatogr., A* **1995**, 702, 3–26.
- Zeng, X. F.; Ruckenstein, E. *Biotechnol. Prog.* **1999**, 15, 1003–1019.
- Klein, E. *J. Membr. Sci.* **2000**, 179, 1–27.
- Charcosset, C. *J. Chem. Technol. Biotechnol.* **1998**, 71, 95–110.
- Bundy, J. L.; Fenselau, C. *Anal. Chem.* **2001**, 73, 751–757.
- Yavuz, H.; Akgol, S.; Arica, Y.; Denizli, A. *Macromol. Biosci.* **2004**, 4, 674–679.
- Morimoto, M.; Saimoto, H.; Usui, H.; Okamoto, Y.; Minami, S.; Shigemasa, Y. *Biomacromolecules* **2001**, 2, 1133–1136.
- Li, X. B.; Tushima, Y.; Morimoto, M.; Saimoto, H.; Okamoto, Y.; Minami, S.; Shigemasa, Y. *Polym. Adv. Technol.* **2000**, 11, 176–179.
- Lee, Y. C.; Lee, R. T. *Acc. Chem. Res.* **1995**, 28, 321–327.
- Goldstein, I. J.; Hollerman, C. E.; Smith, E. E. *Biochemistry* **1965**, 4, 876–883.
- Hong, M. F.; Cassely, A.; Mechref, Y.; Novotny, M. V. *J. Chromatogr., B* **2001**, 752, 207–216.
- Guo, W.; Ruckenstein, E. *J. Membr. Sci.* **2003**, 211, 101–111.
- Ma, Z.; Kotaki, M.; Ramakrishna, S. *J. Membr. Sci.* **2005**, 265, 115–123.

- (26) Nakamatsu, J.; Torres, F. G.; Troncoso, O. P.; Yuan, M. L.; Boccaccini, A. R. *Biomacromolecules* **2006**, *7*, 3345–3355.
- (27) Gümuşderelioglu, M.; Agi, P. *React. Funct. Polym.* **2004**, *61*, 211–220.
- (28) Geng, X. Y.; Kwon, O. H.; Jang, J. H. *Biomaterials* **2005**, *26*, 5427–5432.
- (29) Ohkawa, K.; Cha, D. I.; Kim, H.; Nishida, A.; Yamamoto, H. *Macromol. Rapid Commun.* **2004**, *25*, 1600–1605.
- (30) Ohkawa, K.; Minato, K.-I.; Kumagai, G.; Hayashi, S.; Yamamoto, H. *Biomacromolecules* **2006**, *7*, 3291–3294.
- (31) Che, A.-F.; Huang, X.-J.; Wang, Z.-G.; Xu, Z.-K. *Aust. J. Chem.* **2008**, *61*, 446–454.
- (32) Ye, P.; Xu, Z. K.; Wu, J.; Innocent, C.; Seta, P. *Biomaterials* **2006**, *27*, 4169–4176.
- (33) Kumar, B. A. V.; Varadaraj, M. C.; Tharanathan, R. N. *Biomacromolecules* **2007**, *8*, 566–572.
- (34) Sun, X. Y.; Chen, H.; Gao, H.; Guo, X. Q. *J. Agric. Food Chem.* **2006**, *54*, 9687–9695.
- (35) Capitán, F.; Alonso, E.; Avidad, R.; Capitán-Vallvey, L. F.; Vilchez, J. L. *Anal. Chem.* **1993**, *65*, 1336–1339.
- (36) Eroğlu, A. E.; Volkán, M.; Ataman, O. Y. *Talanta* **2000**, *53*, 89–101.
- (37) Reyes, J. F. G.; Barrales, P. O.; Díaz, A. M. *Talanta* **2005**, *65*, 1203–1208.
- (38) Claesson, P. M.; Ninham, B. W. *Langmuir* **1992**, *8*, 1406–1412.
- (39) Farina, R. D.; Wilkins, R. G. *Biochim. Biophys. Acta* **1980**, *631*, 428–438.
- (40) Banerjee, S. S.; Chen, D.-H. *Chem. Mater.* **2007**, *19*, 3667–3672.
- (41) Sato, K.; Imoto, Y.; Sugama, J.; Seki, S.; Inoue, H.; Odagiri, T.; Hoshi, T.; Anzai, J.-i. *Langmuir* **2005**, *21*, 797–799.
- (42) Mandal, D. K.; Kishore, N.; Brewer, C. F. *Biochemistry* **1994**, *33*, 1149–1156.

BM800882Z